Stopping power of ions in a magnetized two-temperature plasma

H. B. Nersisyan,* M. Walter, and G. Zwicknagel
Institut für Theoretische Physik II, Universität Erlangen, D-91058 Erlangen, Germany
(Received 10 December 1999)

Using the dielectric theory for a weakly coupled plasma, we investigate the stopping power of an ion in an anisotropic two-temperature electron plasma in the presence of a magnetic field. The analysis is based on the assumption that the energy variation of the ion is much less than its kinetic energy. A general expression for the stopping power is analyzed for weak and strong magnetic fields (i.e., for the electron cyclotron frequency less than and greater than the plasma frequency), and for low and high ion velocities. It is found that the usually velocity independent friction coefficient contains an anomalous term which diverges logarithmically as the projectile velocity approaches zero. The physical origin of this anomalous term is the coupling between the cyclotron motion of the electrons and the long-wavelength, low-frequency fluctuations produced by the projectile ion.

PACS number(s): 52.40.Mj, 34.50.Bw, 52.35.−g

I. INTRODUCTION

The energy loss of ions in a plasma has been a topic of great interest due to its importance for the study of basic interactions of charged particles in real media. Recent applications are electron cooling of heavy ion beams [1–3] and energy transfer for inertial confinement fusion (ICF) (see [4] for an overview). Electron cooling is realized by mixing the ion beam periodically with a cold electron beam of the same average velocity. The interaction length is normally about a few meters, and the electron beam is guided by a magnetic field parallel to its direction of motion. The cooling of the ion beam may then be viewed as an energy loss in the common rest frame of both beams. Similar questions arise in heavy-ion-induced ICF. There a frozen hydrogen pellet is heated and compressed by stopping of ion beams in the surrounding converter. In this case the electrons of the solid state converter are acting like a plasma and absorb the incoming energy.

In the electron cooling process the velocity distribution of the electron beam is highly anisotropic because of the acceleration from the cathode to the cooling section. It can be described by a Maxwell distribution with two different temperatures, a longitudinal $T_\parallel$ and a transverse $T_\perp$ [1–3]. Furthermore, an external, longitudinal magnetic field is needed to guide the electrons from the cathode to and through the electron cooler and to stabilize the anisotropic velocity distribution by suppressing the transverse-longitudinal relaxation.

In the present paper we are interested in the influences of the magnetic field and the temperature anisotropy on the ion beam stopping power. Since the early 1960s several theoretical calculations of the stopping power in a magnetized plasma have been presented [5–14]. Stopping of a fast test particle moving with velocity V much higher than the electron thermal velocity $v_{\rm th}$ was studied in Refs. [5, 6, 8]. The energy loss of a charged particle moving with arbitrary velocity was studied in Ref. [7]. The expression obtained there for the Coulomb logarithm, $\Lambda=\ln(\lambda_D/\rho_\perp)$ (where λ_D is the Debye length and $\rho_\perp$ is the impact parameter for scattering for an angle $\vartheta=\pi/2$), corresponds to the classical description of collisions. In the quantum-mechanical case, the Coulomb logarithm is $\Lambda=\ln(\lambda_D/\lambda_B)$, where λ_B is the de Broglie wavelength of the plasma electrons [15].

In Ref. [10], expressions were derived describing the stopping power of a charged particle in a Maxwellian plasma placed in a classically strong magnetic field ($\lambda_B \ll a_c \ll \lambda_D$, where a_c is the electron Larmor radius), under conditions when scattering must be described quantum mechanically. The calculations were carried out for slow test particles whose velocities satisfy the conditions $(m/m_i)^{1/3} v_{\rm th} < V \ll v_{\rm th}$, where m_i is the mass of the plasma ions and m is the electron mass.

In a recent paper [11], the stopping power in a magnetized plasma was investigated for high-velocity light particles, taking into account the Larmor rotation of a test projectile in a magnetic field. It was shown that the stopping power can exhibit an oscillatory dependence on the magnetic field and that it is much greater than without a magnetic field. More attention has been paid to the stopping power in a strongly magnetized plasma for ions that move along the magnetic field [11–13]. Both uncorrelated [11,13] and correlated [12] situations have been discussed. These investigations have concentrated on the stopping power in an isotropic one-temperature plasma. Extensions to nonlinear effects of ion stopping and temperature anisotropy have been made recently by particle-in-cell (PIC) computer simulation [14], where the case $T_\parallel \ll T_\perp$ has been investigated, which is interesting for the electron cooling process. Here, in the framework of dielectric theory, we will focus on the stopping power at arbitrary temperature anisotropy $T_\perp/T_\parallel$.

The paper is organized as follows. We start in Sec. II by solving the linearized Vlasov-Poisson equations by means of Fourier transformation. This provides the general form of the linearized potential generated in a magnetized Maxwellian plasma by a projectile ion, from which the stopping power is deduced. In Sec. III, we apply our results to a nonmagnetized

*Permanent address: Division of Theoretical Physics, Institute of Radiophysics and Electronics, 1 Alikhanian Brothers Str., Ashtarak-2, 378410, Armenia.

plasma. Calculations are carried out for small projectile velocities at arbitrary temperature anisotropy and arbitrary direction of ion motion with respect to the anisotropy axis. Then we turn to the effect of a weak magnetic field on the stopping power in Sec. IV, while we concentrate on the influence of a strong magnetic field in Sec. V. In contrast with the papers [11,13] we consider ion motion in an arbitrary direction. As the last issue we investigate in Sec. VI the stopping power for small projectile velocities at arbitrary magnetic field and temperature anisotropy. The friction coefficient there contains an anomalous term which increases logarithmically when the projectile velocity approaches zero. The results achieved are finally summarized and discussed in Sec. VII.

II. DIELECTRIC THEORY

For the anisotropic plasma with two different temperatures $T_\parallel$ and $T_\perp$ of the electrons we define an average temperature $\overline{T}=\frac{1}{3}T_\parallel+\frac{2}{3}T_\perp$. Within dielectric theory, the electron plasma is described as a continuous, polarizable fluid (medium), which is represented by the phase-space density of the electrons $f(\mathbf{r},\mathbf{v},t)$. Here, only a mean-field interaction between the electrons is considered, and hard collisions are neglected. The evolution of the distribution function $f(\mathbf{r},\mathbf{v},t)$ is determined by the Vlasov-Poisson equation. This is valid for weakly coupled plasmas where the number of electrons in the Debye sphere, $N_D=4\pi n_0\overline{\lambda}_D^3\gg 1$, is very large. Here n_0 is the electron density and $\overline{\lambda}_D=(k_B\overline{T}/4\pi n_0 e^2)^{1/2}$ is an averaged Debye length.

In the following, we consider a nonrelativistic projectile ion with charge Ze and with a velocity $\mathbf{V}$ which moves in a magnetized anisotropic two-temperature plasma at an angle ϑ with respect to the magnetic field $\mathbf{B}_0$. The axis defined by $\mathbf{B}_0$ also coincides with the degree of freedom of temperature $T_\parallel$. We assume that the energy variation of the ion is much smaller than its kinetic energy. We ignore any role of the electron spin or magnetic moment due to the nonrelativistic motion of the ion and the plasma electrons. The strength of the coupling between an ion moving with velocity V and the electron plasma is given by the coupling parameter

$$\mathcal{Z}=\frac{|Z|}{N_D(1+V^2/\overline{v}_{\rm th}^2)^{3/2}}. \tag{1}$$

Here $\overline{v}_{\rm th}=(k_B\overline{T}/m)^{1/2}$ is the average thermal velocity of an electron. The derivation of Eq. (1) is discussed in detail in Ref. [16]. The parameter $\mathcal{Z}$ characterizes the ion-target coupling, where $\mathcal{Z}\ll 1$ corresponds to weak, almost linear coupling and $\mathcal{Z}\gtrsim 1$ to strong, nonlinear coupling.

For a sufficiently small perturbation ($\mathcal{Z}\ll 1$) the linearized Vlasov equation of the plasma may be written as

$$\frac{\partial f_1}{\partial t}+\mathbf{v}\frac{\partial f_1}{\partial \mathbf{r}}-\omega_c(\mathbf{v}\times\mathbf{b})\frac{\partial f_1}{\partial \mathbf{v}}=-\frac{e}{m}\frac{\partial\varphi}{\partial\mathbf{r}}\frac{\partial f_0}{\partial\mathbf{v}}, \tag{2}$$

where $f=f_0+f_1$ and the self-consistent electrostatic potential φ is determined by the Poisson equation

$$\nabla^2\varphi=-4\pi Ze\,\delta(\mathbf{r}-\mathbf{V}t)+4\pi e\int d\mathbf{v}\,f_1(\mathbf{r},\mathbf{v},t). \tag{3}$$

$\mathbf{b}$ is the unit vector parallel to $\mathbf{B}_0$, $-e$ and $\omega_c=eB_0/mc$ are the charge and Larmor frequency of the plasma electrons, respectively, and f_0 is the unperturbed distribution function of plasma electrons, which is here given by two Maxwellians for the longitudinal and transverse degrees of freedom,

$$f_0(v_\parallel,v_\perp)=\frac{n_0}{(2\pi)^{3/2}v_{\rm th\perp}^2 v_{\rm th\parallel}}\exp\left(-\frac{v_\perp^2}{2v_{\rm th\perp}^2}\right)\exp\left(-\frac{v_\parallel^2}{2v_{\rm th\parallel}^2}\right), \tag{4}$$

where $\langle v_\parallel^2\rangle=v_{\rm th\parallel}^2=k_BT_\parallel/m$ and $\langle v_\perp^2\rangle=2v_{\rm th\perp}^2=2k_BT_\perp/m$.

By solving Eqs. (2) and (3) in space-time Fourier components, we obtain the electrostatic potential

$$\varphi(\mathbf{r},t)=\frac{Ze}{2\pi^2}\int d\mathbf{k}\frac{\exp[i\mathbf{k}\cdot(\mathbf{r}-\mathbf{V}t)]}{k^2\varepsilon(\mathbf{k},\mathbf{k}\cdot\mathbf{V})}, \tag{5}$$

which provides the dynamic response of the plasma to the motion of the projectile ion in the presence of the external magnetic field. The dielectric function $\varepsilon(\mathbf{k},\omega)$ of a homogeneous, magnetized, and anisotropic plasma is given by

$$\begin{aligned}\varepsilon(\mathbf{k},\omega)&=1+\frac{1}{k^2\lambda_{D\parallel}^2}[G(s)+iF(s)]\\&=1+\frac{1}{k^2\lambda_{D\parallel}^2}\Bigg[1+is\sqrt{2}\int_0^\infty dt\exp[ist\sqrt{2}-X(t)]\\&\quad+\frac{kv_{\rm th\parallel}\sqrt{2}}{\omega_c}\sin^2\alpha(1-\tau)\int_0^\infty dt\sin\left(\frac{\omega_c t\sqrt{2}}{kv_{\rm th\parallel}}\right)\\&\quad\times\exp[ist\sqrt{2}-X(t)]\Bigg]\end{aligned} \tag{6}$$

with

$$X(t)=t^2\cos^2\alpha+k^2a_c^2\sin^2\alpha\left[1-\cos\left(\frac{\omega_c t\sqrt{2}}{kv_{\rm th\parallel}}\right)\right], \tag{7}$$

where $\lambda_{D\parallel}=v_{\rm th\parallel}/\omega_p$, ω_p is the plasma frequency, $s=\omega/kv_{\rm th\parallel}$, $\tau=T_\perp/T_\parallel$, $a_c=v_{\rm th\perp}/\omega_c$, and α is the angle between the wave vector $\mathbf{k}$ and the magnetic field.

As shown in Appendix A, Eqs. (6) and (7) are identical with the Bessel function representation of $\varepsilon(\mathbf{k},\omega)$ derived, e.g., by Ichimaru [17]. Equations (6) and (7) are, however, more convenient when studying the weak and strong magnetic field limits in Secs. IV and V.

The stopping power S of an ion is defined as the energy loss of the ion in a unit length due to interactions with the plasma electrons. From Eq. (5) it is straightforward to calculate the electric field $\mathbf{E}=-\nabla\varphi$, and the stopping force acting on the ion. Then, the stopping power of the projectile ion becomes

$$S=-\frac{dE}{dl}=Ze\frac{\partial}{\partial\mathbf{r}}\varphi(\mathbf{r},t)\bigg|_{\mathbf{r}=\mathbf{v}t}$$
$$=\frac{2Z^2e^2\lambda_{D\|}^2}{\pi^2}\int_0^{k_{\max}}k^3dk\int_0^1 d\mu\int_0^{\pi}$$
$$\times d\varphi\frac{\cos\Theta F(s)}{[k^2\lambda_{D\|}^2+G(s)]^2+F^2(s)}, \tag{8}$$

where $\mu=\cos\alpha$ is the angle between $\mathbf{k}$ and $\mathbf{B}_0$, Θ is the angle between $\mathbf{k}$ and $\mathbf{V}$, $s=\mathbf{k}\cdot\mathbf{V}/kv_{\mathrm{th}\|}=(V/v_{\mathrm{th}\|})\cos\Theta$, $\cos\Theta=\mu\cos\vartheta-\sqrt{1-\mu^2}\sin\vartheta\cos\varphi$, and ϑ is the angle between $\mathbf{V}$ and $\mathbf{B}_0$. In Eq. (8) we introduced a cutoff parameter $k_{\max}=1/r_{\min}$ (where $r_{\min}$ is the effective minimum impact parameter) in order to avoid the logarithmic divergence at large k. This divergence corresponds to the incapability of the linearized Vlasov theory to treat close encounters between the projectile ion and the plasma electrons properly. For $r_{\min}$ we thus use the effective minimum impact parameter of classical binary Coulomb collisions $r_{\min}=Ze^2/mv_r^2$ for relative velocities $v_r\simeq(V^2+\overline{v}_{\mathrm{th}}^2)^{1/2}$, which is often called the ''distance of closest approach.'' Hence

$$k_{\max}=\frac{1}{r_{\min}}=\frac{m(V^2+\overline{v}_{\mathrm{th}}^2)}{Ze^2}. \tag{9}$$

A two-temperature description of an electron plasma is valid only when the ion beam–plasma interaction time is less than the relaxation time between the two temperatures $T_{\|}$ and $T_{\perp}$. For an estimate we will briefly consider the field-free case, because the external magnetic field suppresses the relaxation between the transverse and longitudinal temperatures during the time of flight of the ion beam through the plasma.

The problem of a temperature relaxation in an anisotropic plasma with and without an external magnetic field was considered by Ichimaru [17]. Within the dominant-term approximation, the relaxation time $\Delta\tau_{\mathrm{rel}}$ for the plasma without magnetic field is given by

$$\frac{1}{\Delta r_{\mathrm{rel}}}=\tfrac{8}{15}\sqrt{\pi/m}\frac{n_0e^4}{(k_BT_{\mathrm{eff}})^{3/2}}\ln\Lambda_c, \tag{10}$$

where $\ln\Lambda_c=\ln(N_D)$ is the Coulomb logarithm and the effective electron temperature T_{eff} is defined through

$$\frac{1}{T_{\mathrm{eff}}^{3/2}}=\tfrac{15}{2}\int_0^1\frac{\mu^2(1-\mu^2)d\mu}{[\mu^2T_{\|}+(1-\mu^2)T_{\perp}]^{3/2}}$$
$$=\frac{5\sqrt{3}}{12\overline{T}^{3/2}}\frac{(1+2\tau)^{3/2}}{(\tau-1)^2}\left[\frac{\tau+2}{\sqrt{|\tau-1|}}p_0(\tau)-3\right], \tag{11}$$

$$p_0(\tau)=\begin{cases}\ln\dfrac{1+\sqrt{1-\tau}}{\sqrt{\tau}}, & \tau<1\\ \arctan\sqrt{\tau-1}, & \tau>1.\end{cases} \tag{12}$$

The relaxation times calculated from Eq. (11) are of the order of 10^{-6}, 0.5×10^{-5}, and 10^{-3} s for averaged temperatures $\overline{T}=10^{-2}$, 0.1, and 1 eV, respectively, for anisotropies $\tau\simeq0.01-100$. The interaction time (for instance, for ICF or for electron cooling) is about $10^{-7}-10^{-8}$ s. Therefore, the ion beam–plasma interaction time can be very small compared to the plasma relaxation time.

III. STOPPING POWER IN PLASMAS WITHOUT MAGNETIC FIELD

Let us analyze expression (8) in the case when a projectile ion moves in an anisotropic two-temperature plasma without a magnetic field. The plasma dielectric function from Eqs. (6) and (7) now takes the form

$$\varepsilon(\mathbf{k},\omega)=1+\frac{1}{k^2\lambda_{D\|}^2}\frac{1}{A^2}W\left(\frac{s}{A}\right). \tag{13}$$

Here $A=[\mu^2+\tau(1-\mu^2)]^{1/2}$ and $W(s)=g_0(s)+if_0(s)$ is the plasma dispersion function [18],

$$g_0(s)=1-s\sqrt{2}\,\mathrm{Di}\left(\frac{s}{\sqrt{2}}\right),\quad f_0(s)=\sqrt{\pi/2}s\exp\left(-\frac{s^2}{2}\right), \tag{14}$$

where

$$\mathrm{Di}(s)=\exp(-s^2)\int_0^s dt\exp(t^2) \tag{15}$$

is the Dawson integral [18], which has for large arguments s the asymptotic behavior $\mathrm{Di}(s)\simeq1/2s+1/4s^3$.

Substituting Eq. (13) into Eq. (8) and performing the k integration we obtain

$$S_0=\frac{Z^2e^2}{2\pi^2\lambda_{D\|}^2}\int_0^1 d\mu\int_0^{\pi}d\varphi\frac{\cos\Theta}{A^2}Q_0\left(\frac{v}{v_{\mathrm{th}\|}}\frac{\cos\Theta}{A},\xi_{\|}A\right), \tag{16}$$

where $\xi_{\|}=k_{\max}\lambda_{D\|}$ and

$$Q_0(x,\xi)=f_0(x)\ln\frac{f_0^2+[\xi^2+g_0(x)]^2}{f_0^2(x)+g_0^2(x)}$$
$$+2g_0(x)\left(\arctan\frac{g_0(x)}{f_0(x)}-\arctan\frac{\xi^2+g_0(x)}{f_0(x)}\right). \tag{17}$$

In the case of an isotropic plasma ($T_{\perp}=T_{\|}\equiv T$ and $\tau=1$) $A=1$, and Eq. (16) coincides with the result of, e.g., Ref. [19]:

$$S_0=\frac{Z^2e^2}{2\pi\lambda_D^2}\frac{v_{\mathrm{th}}^2}{V^2}\int_0^{V/v_{\mathrm{th}}}d\mu\,\mu Q_0(\mu,\xi), \tag{18}$$

where $v_{\mathrm{th}}=v_{\mathrm{th}\|}=v_{\mathrm{th}\perp}$, $\lambda_D=v_{\mathrm{th}}/\omega_p$, and $\xi=k_{\max}\lambda_D$.

When a projectile ion moves slowly through a plasma, the electrons have much time to experience the ion attractive potential. They are accelerated toward the ion, but when they reach its trajectory the ion has already moved forward a little bit. Hence, we expect an increased density of electrons at some place in the wake of the ion. This negative charge

density pulls back the positive ion and gives rise to the stopping. This drag force is of particular interest for the electron cooling process. In the limit of small velocities $S \simeq RV$. This looks like the friction law of a viscous fluid, and accordingly R is called the friction coefficient. However, in the case of an ideal plasma it should be noted that this law does not depend on the plasma viscosity and is not a consequence of electron-electron collisions, which are neglected in the Vlasov equation.

The Taylor expansion of Eq. (16) for small V ($V \ll \overline{v}_{\rm th}$) yields the friction law

$$S_0 = \frac{Z^2 (e^2/\overline{\lambda}_D^2)}{3\sqrt{2\pi}} \frac{V}{\overline{v}_{\rm th}} \psi(\overline{\xi}) [I_1(\tau) + I_2(\tau) \sin^2 \vartheta], \quad (19)$$

where $\overline{\xi} = k_{\max} \overline{\lambda}_D = (1 + V^2/\overline{v}_{\rm th}^2)/\mathcal{Z} \simeq 1/\mathcal{Z}$,

$$I_1(\tau) = \frac{3}{\psi(\overline{\xi})} \left(\frac{2\tau + 1}{3} \right)^{3/2} \int_0^1 d\mu \, \frac{\mu^2 \psi(\xi_\parallel A(\mu))}{A^3(\mu)}, \quad (20)$$

$$I_2(\tau) = \frac{3}{2\psi(\overline{\xi})} \left(\frac{2\tau + 1}{3} \right)^{3/2} \int_0^1 d\mu \, \frac{(1 - 3\mu^2) \psi(\xi_\parallel A(\mu))}{A^3(\mu)}, \quad (21)$$

and the function ψ is

$$\psi(\xi) = \ln(1 + \xi^2) - \frac{\xi^2}{1 + \xi^2}. \quad (22)$$

In the case of an isotropic plasma ($\tau = 1$) we have $I_1 = 1$ and $I_2 = 0$ and Eq. (19) becomes the usual friction law [19]. For the case of strong temperature anisotropy, when $\tau \ll 1 (T_\perp \ll T_\parallel)$ we have $\xi_\parallel \simeq \sqrt{3}/\mathcal{Z}$ and

$$I_1 \simeq -\frac{\sqrt{3}}{6\psi(\overline{\xi})} [\mathrm{Li}_2(1 + \xi_\parallel^2) + \ln(1 + \xi_\parallel^2)], \quad (23)$$

$$I_2 \simeq \frac{\sqrt{3}}{12\psi(\overline{\xi})} [\xi_\parallel^2 + 2 \ln(1 + \xi_\parallel^2) + 3 \, \mathrm{Li}_2(1 + \xi_\parallel^2)]. \quad (24)$$

Here the functions I_1 and I_2 do not depend on τ, and $\mathrm{Li}_2(x)$ is the dilogarithm function [20]. Note that $\mathcal{Z} \ll 1$ and therefore $\overline{\xi} \gg 1$, $\xi_\parallel \gg 1$ in Eqs. (23) and (24). The Coulomb logarithms in Eqs. (23) and (24) are then the leading terms and

$$I_1 \simeq \frac{\sqrt{3}}{6} \ln \frac{1}{\mathcal{Z}} \ll I_2 \simeq \frac{\sqrt{3}}{8\mathcal{Z}^2} \frac{1}{\ln(1/\mathcal{Z})}. \quad (25)$$

The normalized friction coefficient [Eq. (19)] is thus dominated by the second term and increases with increasing ϑ.

In the opposite case, $\tau \gg 1 (T_\perp \gg T_\parallel)$, the evaluation of Eqs. (20) and (21) yields

$$I_1 \simeq \frac{\pi\sqrt{6}}{3\psi(\overline{\xi})} \left(\sqrt{1 + \tfrac{3}{2}\overline{\xi}^2} - 1 - 2 \ln \frac{1 + \sqrt{1 + \frac{3}{2}\overline{\xi}^2}}{2} \right), \quad (26)$$

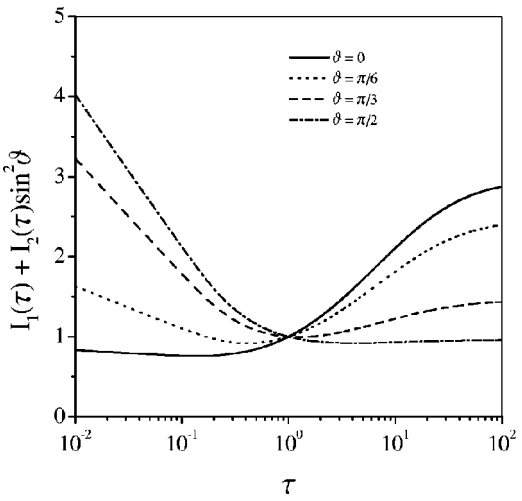

FIG. 1. Normalized friction coefficient $I_1 + I_2 \sin^2 \vartheta$ [see Eqs. (19)–(21)] in plasma with $\mathcal{Z} = 0.2$ as a function of $\tau = T_\perp / T_\parallel$ for four values of ϑ: $\vartheta = 0$ (solid line), $\pi/6$ (dotted line), $\pi/3$ (dashed line), and $\pi/2$ (dot-dashed line).

$$I_2 \simeq \frac{\pi\sqrt{6}}{6\psi(\overline{\xi})} \left(1 + \frac{1}{\sqrt{1 + \frac{3}{2}\overline{\xi}^2}} - 2\sqrt{1 + \tfrac{3}{2}\overline{\xi}^2} + 6 \ln \frac{1 + \sqrt{1 + \frac{3}{2}\overline{\xi}^2}}{2} \right), \quad (27)$$

and

$$I_1 \simeq -I_2 \simeq \frac{\pi}{2\mathcal{Z}\ln(1/\mathcal{Z})}. \quad (28)$$

Then $I_1 + I_2 \sin^2 \vartheta \simeq I_1 \cos^2 \vartheta$ and the normalized friction coefficient decreases with increasing ϑ in this case.

In Fig. 1 the normalized friction coefficient $I_1 + I_2 \sin^2 \vartheta$ is plotted as a function of temperature anisotropy τ for $\vartheta = 0$ (solid line), $\pi/6$ (dotted line), $\pi/3$ (dashed line), and $\pi/2$ (dot-dashed line), and for fixed plasma density and average temperature ($\mathcal{Z} = 0.2$). Figure 1 shows an enhancement of the friction coefficient when the ion moves along the direction with low temperature. This effect can easily be explained in a binary collision picture. Let us consider the particular case of a strongly anisotropic plasma $T_\perp \gg T_\parallel$. In this case the plasma electrons move mostly in the direction across the anisotropy axis. For $\vartheta \simeq \pi/2$ the projectile ion moves along the direction of the plasma electron thermal fluctuations and the effective impact parameter for electron-ion collision is very small. Thus the friction coefficient decreases. For $\vartheta \simeq 0$ the projectile ion moves perpendicular to the direction of the plasma electron thermal fluctuations. Therefore, the impact parameter for electron-ion collisions increases, which raises the friction coefficient.

For arbitrary projectile velocities we evaluated Eq. (16) numerically. In Figs. 2 and 3 the stopping power is plotted for plasmas with large temperature anisotropy ($\tau = 10^{-2}$ and $\tau = 10^2$ in Figs. 2 and 3, respectively) with $n_0 = 10^8 \, \mathrm{cm}^{-3}$, $\overline{T} = 0.1 \, \mathrm{eV}$, and for four values of ϑ; $\vartheta = 0$ (dotted line), $\pi/6$

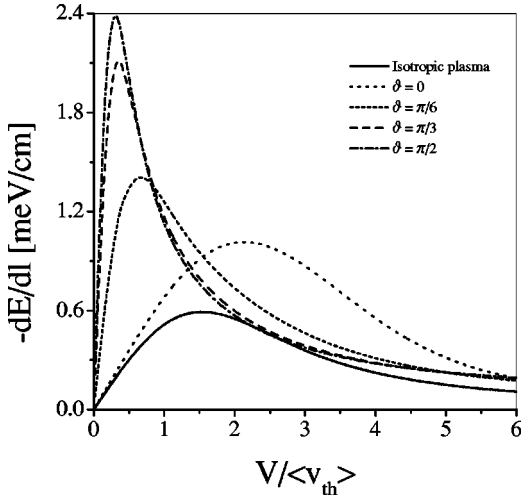

FIG. 2. Stopping power (in units of meV/cm) as a function of the projectile velocity V (in units of $\langle v_{\rm th}\rangle=\overline{v_{\rm th}}$) in a plasma with large temperature anisotropy without magnetic field ($\overline{T}=0.1$ eV, $n_0=10^8$ cm^{-3}, $\tau=10^{-2}$) for four values of the angle ϑ: $\vartheta=0$ (dotted line), $\pi/6$ (short-dashed line), $\pi/3$ (dashed line), and $\pi/2$ (dot-dashed line). Solid line: isotropic plasma with temperature $T=\overline{T}=0.1$ eV.

(short-dashed line), $\pi/3$ (dashed line), and $\pi/2$ (dot-dashed line). The solid lines are plotted for an isotropic one-temperature plasma with $T=\overline{T}=0.1$ eV. The general behavior of the stopping power for two anisotropy parameters τ is characterized by an increase by comparison with the isotropic case. At $\vartheta\simeq\pi/2$ and $\tau=10^{-2}$ (Fig. 2) the ion moves in the direction across the longitudinal electron motion with the lower temperature $T_\perp$ and the maximum of the stopping power is around $V\simeq v_{\rm th\perp}$, whereas the maximum for ion motion in the longitudinal direction is at $V\simeq v_{\rm th\|}\gg v_{\rm th\perp}$.

IV. STOPPING IN PLASMAS WITH WEAK MAGNETIC FIELD

For the case when the magnetic field is weak, in the sense that the dimensionless parameter $\eta=\omega_c/\omega_p$ is much less than unity, the functions G and F [Eqs. (6) and (7)], which

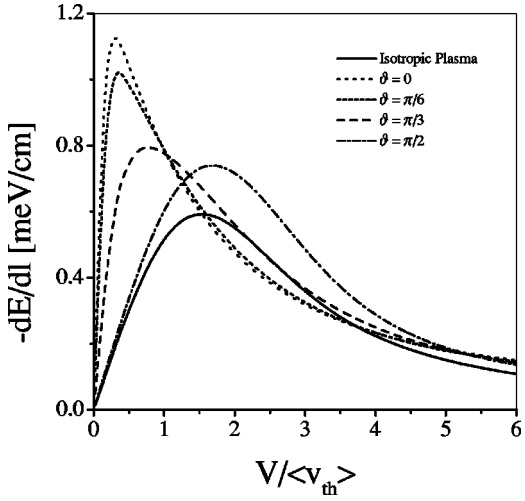

FIG. 3. As Fig. 2, but here $\tau=10^2$.

define the dielectric function, can be expanded about their field-free values $g_0(s/A)/A^2$, $f_0(s/A)/A^2$ [Eqs. (14) and (15)] as

$$G(s)+iF(s)=\frac{1}{A^2}\left[g_0\left(\frac{s}{A}\right)+if_0\left(\frac{s}{A}\right)\right]+\eta^2\frac{\sin^2\alpha}{(k\lambda_{D\|})^2}[g_1(s)+if_1(s)], \quad (29)$$

where

$$g_1(s)+if_1(s)=\tfrac{2}{3}(1-\tau)\int_0^\infty t^3dt\left(\frac{t^2}{2}\tau\sin^2\alpha-1\right)\times\exp(ist\sqrt{2}-A^2t^2)+\frac{is\sqrt{2}}{6}\tau\int_0^\infty t^4dt\exp(ist\sqrt{2}-A^2t^2), \quad (30)$$

$s=\omega/kv_{\rm th\|}$. Substituting expressions (29) and (30) into Eq. (8) leads to

$$S=S_0+\eta^2S_1, \quad (31)$$

where S_0 is the stopping power in plasmas without magnetic field [Eq. (16)] and η^2S_1 represents the change due to a weak magnetic field. After some simplifications this becomes

$$S_1=\sqrt{\pi/2}\frac{Z^2e^2}{24\pi^2\lambda_{D\|}^2}\frac{V}{v_{\rm th\|}}\int_0^1d\mu\int_0^\pi d\varphi\frac{(1-\mu^2)\cos^2\Theta}{A^5}\times\exp\left(-\frac{V^2}{v_{\rm th\|}^2}\frac{\cos^2\Theta}{2A^2}\right)\times\frac{\tau[7-(V^2/u_{\rm th\|}^2)(\cos^2\Theta/A^2)]-4A^2}{f_0^2[(V/u_{\rm th\|})(\cos\Theta/A)]+g_0^2[(V/u_{\rm th\|})(\cos\Theta/A)]}. \quad (32)$$

In the isotropic plasma ($\tau=1$) Eq. (32) coincides with the results by May and Cramer [7] after integration over φ. Note that the additional term S_1 does not depend on the cutoff parameter $k_{\rm max}$.

In the next subsections we evaluate Eq. (32) for small and large projectile velocities.

A. Small projectile velocities

When the projectile ion moves slowly ($V<\overline{v_{\rm th}}$) in the plasma, Eq. (32) leads to the simplified expression

$$S_1=\frac{Z^2e^2}{60\pi\overline{\lambda}_D^2}\sqrt{\pi/2}\frac{V}{\overline{v}_{\rm th}}P(\vartheta,\tau), \quad (33)$$

with

$$P(\vartheta,\tau)=\left(\frac{1+2\tau}{3}\right)^{3/2}[P_1(\tau)+P_2(\tau)\sin^2\vartheta], \quad (34)$$

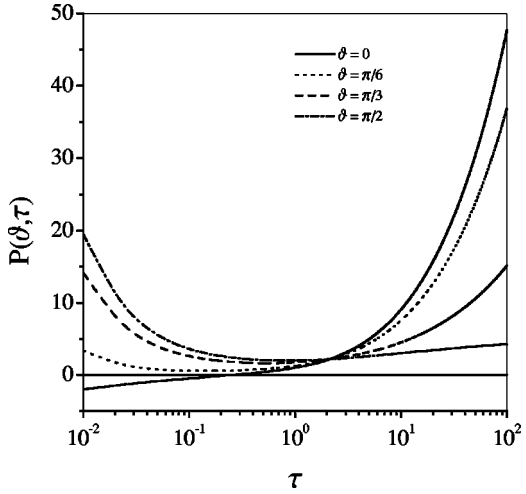

FIG. 4. The function $P(\vartheta,\tau)$ [see Eqs. (33)–(36)] as a function of $\tau=T_\perp/T_\parallel$ for four values of ϑ: $\vartheta=0$ (solid line), $\pi/6$ (dotted line), $\pi/3$ (dashed line), and $\pi/2$ (dot-dashed line).

$$P_1(\tau)=\frac{5}{6(1-\tau)^2}\left(14\tau+25-\frac{3(9\tau+4)}{\sqrt{|1-\tau|}}p_0(\tau)\right), \quad (35)$$

$$P_2(\tau)=\frac{5}{12\tau(1-\tau)^2}\left(\frac{3\tau(23\tau+16)}{\sqrt{|1-\tau|}}\times p_0(\tau)-28\tau^2-91\tau+2\right). \quad (36)$$

Here, the function $p_0(\tau)$ is given by Eq. (12). In an isotropic plasma with $\tau=1$ we have $P_1(1)=P_2(1)=1$.

In Fig. 4 the normalized friction coefficient $P(\vartheta,\tau)$ for the additional stopping power S_1 is plotted as a function of τ for $\vartheta=0$ (solid line), $\pi/6$ (dotted line), $\pi/3$ (dashed line), and $\pi/2$ (dot-dashed line). The general behavior of $P(\vartheta,\tau)$ is similar to the friction coefficient of the plasma without magnetic field (see Fig. 1). Here, the correction $P(\vartheta,\tau)$ can also be negative at small τ and ϑ, which then corresponds to a slight decrease of the stopping power, Eq. (31).

B. High projectile velocities

When the projectile ion moves with large velocity ($V\gg\overline{v_{\rm th}}$), Eq. (32) yields

$$S_1\simeq-\frac{Z^2e^2\omega_p^2}{4V^2}(1+\cos^2\vartheta). \quad (37)$$

This result is in accord with the results of Honda, Aona, and Kihara [6] and May and Cramer [7], who, however, kept the terms $O(V^{-4})$ in their work as well. Although the function S_1 in Eq. (37) is proportional to the plasma density, the full correction term $\eta^2 S_1$ does not depend on the plasma density.

In Figs. 5 and 6 we show the velocity dependence of the function S_1 for $\tau=10^{-2}$ and 10^2, respectively. The different curves are $\vartheta=0$ (solid line), $\pi/6$ (dotted line), $\pi/3$ (dashed line), and $\pi/2$ (dot-dashed line). For small and medium projectile velocities the weak magnetic field decreases the total stopping power for small τ and increases it in the high-τ limit. For high projectile velocities the magnetic field always reduces the stopping power independent of the temperature anisotropy; see Eq. (37).

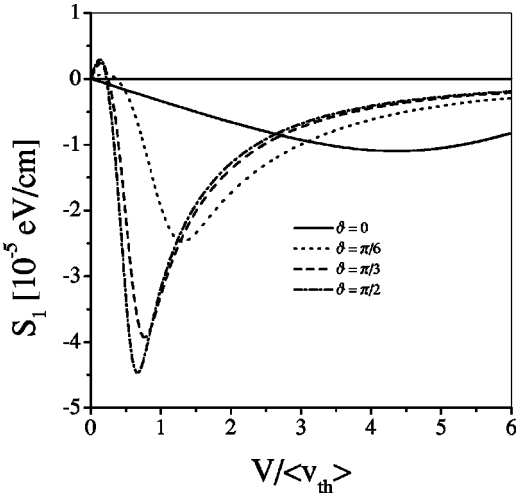

FIG. 5. Additional stopping power S_1 (in 10^{-5} eV/cm) in plasma ($n_0=10^8\,{\rm cm}^{-3}$, $\overline{T}=0.1$ eV, $\tau=10^{-2}$) with weak magnetic field [see Eq. (32)] as a function of projectile velocity V (in units of $\langle v_{\rm th}\rangle=\overline{v_{\rm th}}$) for $\vartheta=0$ (solid line), $\pi/6$ (dotted line), $\pi/3$ (dashed line), and $\pi/2$ (dot-dashed line).

V. STOPPING IN PLASMAS WITH STRONG MAGNETIC FIELD

We now turn to the case when a projectile ion moves in an anisotropic plasma with a strong magnetic field, which is, on one hand, sufficiently weak to allow a classical description ($\hbar\omega_c<k_BT_\perp$ or $\hbar/mv_{\rm th\perp}<a_c$), and, on the other hand, comparatively strong so that the cyclotron frequency of the plasma electrons exceeds the plasma frequency $\omega_c\gg\omega_p$. This limits the values of the magnetic field, the perpendicular temperature, and the plasma density. From these conditions we can obtain

$$3\times10^{-6}n_0^{1/2}<B_0<10^5T_\perp, \quad (38)$$

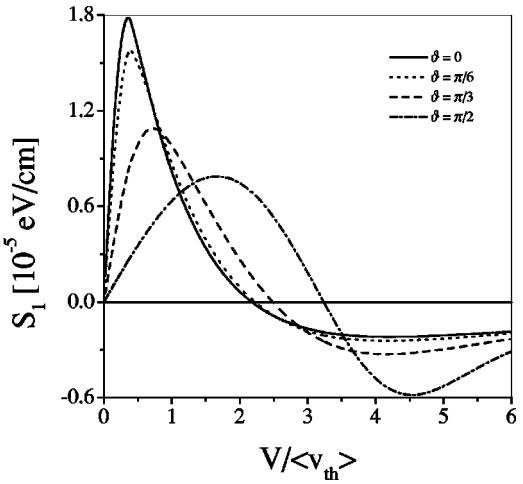

FIG. 6. As Fig. 5, but here $\tau=10^2$.

where n_0 is measured in cm^{-3}, $T_\perp$ in eV, and B_0 in kG. Conditions (38) are always true in the range of parameters $n_0 < 10^{15}\,\mathrm{cm}^{-3}$, $B_0 < 100\,\mathrm{kG}$, and $T_\perp > 10^{-3}\,\mathrm{eV}$. Then the perpendicular motion of the electrons is completely quenched and the stopping power depends only on the longitudinal electron temperature $T_\parallel$. The dependence on the transverse temperature will be introduced only by the cutoff parameter Eq. (9).

In the limit of sufficiently strong magnetic field, Eq. (8) becomes

$$S_{\mathrm{inf}} = \frac{2Z^2e^2}{\pi^2\lambda_{D\parallel}^2}\int_0^{\xi_\parallel} k^3 dk \int_0^1 d\mu \int_0^\pi d\varphi \frac{\cos\Theta f_0(s)}{[k^2+g_0(s)]^2+f_0^2(s)}, \tag{39}$$

with $s=(V/u_{\mathrm{th}\parallel})(\cos\Theta/\mu)$ and g_0, f_0 from Eqs. (14), which gives after integration over k

$$S_{\mathrm{inf}} = \frac{Z^2e^2}{2\pi^2\lambda_{D\parallel}^2}\int_0^1 d\mu \int_0^\pi d\varphi \cos\Theta Q_0\left(\frac{V}{v_{\mathrm{th}\parallel}}\frac{\cos\Theta}{\mu}, \xi_\parallel\right). \tag{40}$$

Here the function Q_0 is given by Eq. (17). For further simplification of Eq. (40) we introduce the new variable of integration $x=\cos\Theta/\mu$. After φ integration in Eq. (40) we finally find the stopping power in the presence of a strong magnetic field as

$$S_{\mathrm{inf}}(V,\vartheta) = \frac{Z^2e^2}{8\pi\lambda_{D\parallel}^2} Q\left(\frac{V}{v_{\mathrm{th}\parallel}}, \vartheta\right), \tag{41}$$

where

$$Q\left(\frac{V}{v_{\mathrm{th}\parallel}}, \vartheta\right) = \sin^2\vartheta \int_{-\infty}^{\infty} \frac{Q_0[(V/v_{\mathrm{th}\parallel})x, \xi_\parallel]x\,dx}{(x^2+1-2x\cos\vartheta)^{3/2}}. \tag{42}$$

In previous work [11–13] only the case of $\vartheta=0$ (the motion of the projectile along the magnetic field direction) has been investigated. In this case the integral in Eq. (42) diverges, while the prefactor $\sin^2\vartheta$ tends to zero. Introducing the new variable of integration in Eq. (42), $y=(x-\cos\vartheta)/\sin\vartheta$, we obtain for vanishing angle ϑ

$$Q\left(\frac{V}{v_{\mathrm{th}\parallel}}, \vartheta\to 0\right) = 2Q_0\left(\frac{V}{v_{\mathrm{th}\parallel}}, \xi_\parallel\right). \tag{43}$$

Thus expression (41) reproduces the known results for the stopping power on an ion which moves along the direction of the magnetic field [11–13].

In the following paragraphs we will discuss its low- and high-velocity limits.

A. Small projectile velocities

In the low-velocity limit ($V \ll v_{\mathrm{th}\parallel}$) Eq. (42) becomes

$$Q\left(\frac{V}{v_{\mathrm{th}\parallel}}, \vartheta\right) \simeq \frac{2V}{v_{\mathrm{th}\parallel}}\left\{\sqrt{2\pi}\psi(\xi_\parallel)\left[\sin^2\vartheta \ln\left(\frac{2v_{\mathrm{th}\parallel}}{V\sin\vartheta}\right) + 1 - 2\sin^2\vartheta\right] + C_1(\xi_\parallel)\sin^2\vartheta\right\}, \tag{44}$$

where

$$C_1(\xi_\parallel) = \int_0^1 \frac{dx}{x^2}[Q_0(x,\xi_\parallel) - \sqrt{2\pi}\psi(\xi_\parallel)x] + \int_1^\infty \frac{dx}{x^2} Q_0(x,\xi_\parallel). \tag{45}$$

Here, the function ψ is defined by Eq. (22). Since we deal with small ion beam–plasma coupling $\mathcal{Z} \ll 1$ we have $\xi_\parallel \gg 1$ in Eqs. (44) and (45) and the function $C_1(\xi)$ simplifies to

$$C_1(\xi_\parallel) \simeq \sqrt{2\pi}\ln\frac{2}{\gamma}\ln\xi_\parallel + 0.6, \tag{46}$$

where $\gamma = 0.5772$ is Euler's constant.

We note that the friction coefficient S_{inf}/V from Eqs. (41) and (44) contains a term which depends logarithmically on V and which vanishes for $\vartheta\to 0$. It will be shown in the next section that this behavior is a characteristic feature of the stopping power at low velocities for arbitrary strength of the magnetic field.

B. High projectile velocities

In the case of high projectile velocities ($V \gg v_{\mathrm{th}\parallel}$) the general expression (42) becomes

$$Q\left(\frac{V}{v_{\mathrm{th}\parallel}}, \vartheta\right) \simeq \frac{4\pi v_{\mathrm{th}\parallel}^2}{V^2}\left\{\sin^2\vartheta\left[\ln\left(\frac{2V}{v_{\mathrm{th}\parallel}\sin\vartheta}\right) + C_2(\xi_\parallel) - 2\right] + 1\right\}, \tag{47}$$

where

$$C_2(\xi_\parallel) = \frac{1}{2\pi}\int_0^1 Q_0(x,\xi_\parallel)x\,dx + \int_1^\infty \frac{dx}{x}\left[\frac{x^2}{2\pi}Q_0(x,\xi_\parallel) - 1\right], \tag{48}$$

which gives for $\xi_\parallel \gg 1$ $C_2(\xi_\parallel) \simeq \ln\xi_\parallel$. The stopping power for strong magnetic fields shows, in the low- and high-velocity limits [Eqs. (44) and (47)], an enhancement for ions moving transverse to the magnetic field compared to the case of the longitudinal motion ($\vartheta=0$). This effect is in agreement with PIC simulation results [14]. In contrast to the field-free case, at strong magnetic field and for $\vartheta=0$, $V \gg u_{\mathrm{th}\parallel}$ [Eqs. (41) and (47)] $S_{\mathrm{inf}} \simeq Z^2e^2\omega_p^2/2V^2$ is independent of $k_{\max}$. The cutoff $k_{\max}$, necessary at low ion velocities, is, however, less well defined here than for the field-free case, where the cutoff (9) was deduced from the binary collision picture. Now, the electrons are forced to move parallel to $\mathbf{B}_0$. Since we assumed the motion of the ion in this direction as well, the ion and an electron just pass each other along a straight line. For symmetry reasons the total momentum transfer and the stopping power are zero. Purely binary interactions contribute nothing and the stopping of the ion is due only to the collective response of the plasma, that is, due to modes with long wavelengths $k < 1/\lambda_{D\parallel}$. This suggests taking $k_{\max}$ of the order of $1/\lambda_{D\parallel}$, but further investigations are clearly needed here for a more precise description in this particular case.

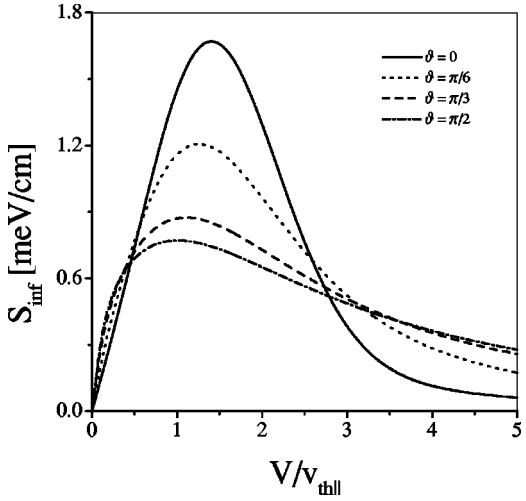

FIG. 7. Stopping power $S_{\rm inf}$ (in meV/cm) in plasma ($n_0 = 10^6\,{\rm cm}^{-3}$, $T_\| = 10^{-4}$ eV, $\tau = 0.1$) with strong magnetic field as a function of projectile velocity V (in units of $v_{\rm th\|}$) for $\vartheta = 0$ (solid line), $\pi/6$ (dotted line), $\pi/3$ (dashed line), and $\pi/2$ (dot-dashed line).

In Figs. 7 and 8, the stopping power $S_{\rm inf}$ is plotted as a function of projectile velocity (in units of $v_{\rm th\|}$) for $n_0 = 10^6\,{\rm cm}^{-3}$, $T_\| = 10^{-4}$ eV, and $T_\perp = 10^{-5}$ eV (Fig. 7), $T_\perp = 0.1$ eV (Fig. 8), and for four different values of the angle ϑ: $\vartheta = 0$ (solid line), $\pi/6$ (dotted line), $\pi/3$ (dashed line), and $\pi/2$ (dot-dashed line). The enhancement of $S_{\rm inf}(V,\vartheta)$ with respect to $S_{\rm inf}(V,0)$ in the low-and high-velocity limits by increasing the angle ϑ is documented in Fig. 9, for $T_\| = 10^{-4}$ eV, $T_\perp = 0.1$ eV, $n_0 = 10^6\,{\rm cm}^{-3}$, and $\vartheta = \pi/6$ (solid line), $\pi/4$ (dotted line), $\pi/3$ (dashed line), and $\pi/2$ (dot-dashed line). The physical origin of this angular behavior in the low- and high-velocity limits is the enhancement of the effective impact parameter for an individual electron-ion collision with increasing ϑ. For medium projectile velocities $V \simeq v_{\rm th\|}$ the collective excitations in the plasma become important and thus the stopping power is higher for small ϑ.

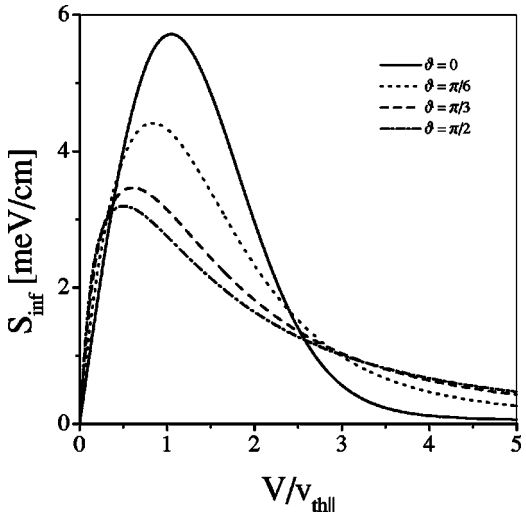

FIG. 8. As Fig. 7, but here $\tau = 10^3$.

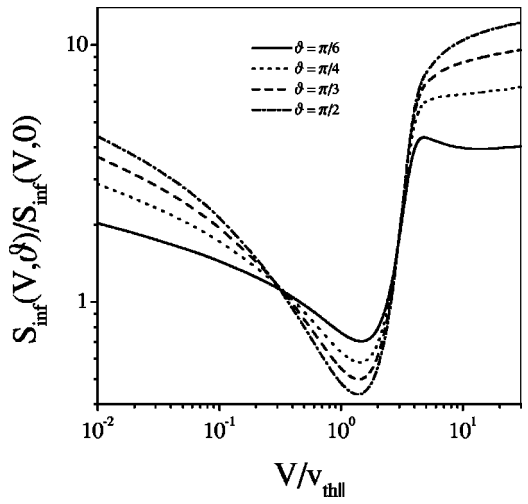

FIG. 9. The ratio $S_{\rm inf}(V,\vartheta)/S_{\rm inf}(V,0)$ as a function of projectile velocity V (in units of $v_{\rm th\|}$) for $T_\| = 10^{-4}$ eV, $\tau = 10^3$, $\vartheta = \pi/6$ (solid line), $\pi/4$ (dotted line), $\pi/3$ (dashed line), and $\pi/2$ (dot-dashed line).

VI. STOPPING AT ARBITRARY MAGNETIC FIELD AND IN LOW-VELOCITY LIMIT: ANOMALOUS FRICTION COEFFICIENT

We now proceed with a projectile ion at low velocities and at arbitrary magnetic field. This regime is of particular importance for the electron cooling process [1–3]. In the presence of a magnetic field the friction coefficient here contains a term that diverges like $\ln(v_{\rm th\|}/V)$ in addition to the usual constant one (see, e.g., Sec. III). For this consideration it is convenient to use the Bessel function representation of the dielectric function, which has been given, e.g., by Ichimaru [17] [see Appendix A, Eq. (A7)] and to write the real and imaginary parts of Eq. (A7) separately,

$$G = 1 - \frac{\sqrt{2}\,\omega}{|k_\||v_{\rm th\|}}\Lambda_0(z)\,{\rm Di}\left(\frac{\omega}{|k_\||v_{\rm th\|}\sqrt{2}}\right) - \frac{\sqrt{2}}{|k_\||v_{\rm th\|}}\sum_{n=1}^{\infty}\Lambda_n(z) \times\left\{\omega\left[{\rm Di}\left(\frac{\omega+n\omega_c}{|k_\||v_{\rm th\|}\sqrt{2}}\right)+{\rm Di}\left(\frac{\omega-n\omega_c}{|k_\||v_{\rm th\|}\sqrt{2}}\right)\right]+n\omega_c\left(\frac{1}{\tau}-1\right) \times\left[{\rm Di}\left(\frac{\omega-n\omega_c}{|k_\||v_{\rm th\|}\sqrt{2}}\right)-{\rm Di}\left(\frac{\omega+n\omega_c}{|k_\||v_{\rm th\|}\sqrt{2}}\right)\right]\right\}, \tag{49}$$

$$F = \sqrt{\pi/2}\left\{\frac{\omega}{|k_\||v_{\rm th\|}}\Lambda_0(z)\exp\left(-\frac{\omega^2}{2k_\|^2v_{\rm th\|}^2}\right) + \frac{2}{|k_\||v_{\rm th\|}}\sum_{n=1}^{\infty}\Lambda_n(z)\exp\left(-\frac{\omega^2+n^2\omega_c^2}{2k_\|^2v_{\rm th\|}^2}\right) \times\left[\omega\cosh\left(\frac{n\omega_c\omega}{k_\|^2v_{\rm th\|}^2}\right)+n\omega_c\left(\frac{1}{\tau}-1\right)\sinh\left(\frac{n\omega_c\omega}{k_\|^2v_{\rm th\|}^2}\right)\right]\right\}. \tag{50}$$

The notations in Eqs. (49) and (50) are explained in Appendix A.

For the friction coefficient we have to consider S, given by Eq. (8) in the low-velocity limit, and thus the functions G

and F given by Eqs. (49) and (50), when $\omega=\mathbf{k}\cdot\mathbf{V}$. Now we have to write the Taylor expansion of Eqs. (49) and (50) for small $\omega=\mathbf{k}\cdot\mathbf{V}$. However, the first term of Eq. (50) exhibits a singular behavior in the limit of $\omega=\mathbf{k}\cdot\mathbf{V}\to 0$ where the $k_\parallel$ integration diverges logarithmically for small $k_\parallel$. We must therefore keep $\omega=\mathbf{k}\cdot\mathbf{V}$ finite in that integration to avoid such a divergence. This anomalous contribution that arises from the first term of Eq. (50) in the low-velocity limit is

$$S_{\rm an}\simeq\left(\frac{2}{\pi^3}\right)^{1/2}\frac{Z^2e^2}{\lambda_{D\parallel}^2}\frac{V}{v_{\rm th\parallel}}\int_0^{\xi_\parallel}k^3dk\int_0^1\frac{d\mu}{\mu}\int_0^\pi d\varphi\cos^2\Theta \times\frac{\Lambda_0(z)\exp[-(V^2/2v_{\rm th\parallel}^2)(\cos^2\Theta/\mu^2)]}{[k^2+E_2(k,\mu)]^2}, \tag{51}$$

where $\Lambda_0(z)=\exp(-z)I_0(z)$, and $E_2(k,\mu)=G(\omega=0)$ is

$$E_2(k,\mu)=1+\frac{2\sqrt{2}\,\eta}{k\mu}\left(\frac{1}{\tau}-1\right)\sum_{n=1}^{\infty}n\Lambda_n(z)\mathrm{Di}\left(\frac{n\eta}{k\mu\sqrt{2}}\right). \tag{52}$$

Here $z=(k^2\tau/\eta^2)(1-\mu^2)$, $\mu=\cos\alpha=k_\parallel/k$, and Θ is the angle between $\mathbf{k}$ and $\mathbf{V}$. After μ and φ integration (see Appendix B), Eq. (51) reads

$$S_{\rm an}\simeq\left(\frac{2}{\pi}\right)^{1/2}\frac{Z^2e^2}{4\lambda_{D\parallel}^2}\frac{V}{v_{\rm th\parallel}}\sin^2\vartheta\ln\left(\frac{v_{\rm th\parallel}}{V}\frac{2.26}{\sin\vartheta}\right)\mathcal{F}(\tau,\eta), \tag{53}$$

with

$$\mathcal{F}(\tau,\eta)=\int_0^{\tau\xi_\parallel^2}\frac{\Lambda_0(x/\eta^2)x\,dx}{[x+1+(\tau-1)\Lambda_0(x/\eta^2)]^2}. \tag{54}$$

The function $\mathcal{F}$ and thus $S_{\rm an}$ [Eq. (53)] vanishes in the limit $B_0\to 0$ (or $\eta\to 0$) like

$$\mathcal{F}(\tau,\eta)\simeq\frac{\eta}{(2\pi)^{1/2}}\left(\arctan(k_{\max}\lambda_{D\perp})-\frac{k_{\max}\lambda_{D\perp}}{1+(k_{\max}\Lambda_{D\perp})^2}\right). \tag{55}$$

The anomalous term Eqs. (53) and (54) therefore represent a new effect arising from the presence of the magnetic field, which is not restricted to anisotropic plasmas.

For an isotropic plasma ($\tau=1$) and for a sufficiently weak magnetic field $\eta<\xi_\parallel$ (or $\omega_c<k_{\max}v_{\rm th\parallel}$), Eq. (54) takes the form

$$\mathcal{F}(\tau,\eta)\simeq\exp\left(\frac{1}{\eta^2}\right)\left[\left(1+\frac{1}{\eta^2}\right)K_0\left(\frac{1}{\eta^2}\right)-\frac{1}{\eta^2}K_1\left(\frac{1}{\eta^2}\right)\right], \tag{56}$$

where K_0 and K_1 are modified Bessel functions of the second kind. In the case of very strong magnetic field $\eta>\xi_\parallel\sqrt{\tau}$ (or $\omega_c>k_{\max}\lambda_{D\perp}$), the function $\mathcal{F}(\tau,\eta)$ reads

$$\mathcal{F}(\tau,\eta)\simeq\Psi(\xi_\parallel)=\ln(1+\xi_\parallel^2)-\frac{\xi_\parallel^2}{1+\xi_\parallel^2}. \tag{57}$$

The physical origin of such an anomalous friction coefficient may be traced to the spiral motion of the electrons along the magnetic field lines. These electrons naturally tend to couple strongly with long-wavelength fluctuations (i.e., small $k_\parallel$) along the magnetic field. In addition, when such fluctuations are characterized by slow variation in time (i.e., small $\omega=\mathbf{k}\cdot\mathbf{V}$), the contact time or the rate of energy exchange between the electrons and the fluctuations will be further enhanced. In a plasma, such low-frequency fluctuations are provided by the slow projectile ion. The above coupling can therefore be an efficient mechanism of energy exchange between the electrons and the projectile ion. In the limit of $V\to 0$, the frequency $\omega=\mathbf{k}\cdot\mathbf{V}\to 0$ tends to zero as well. The contact time thus becomes infinite and the friction coefficient diverges.

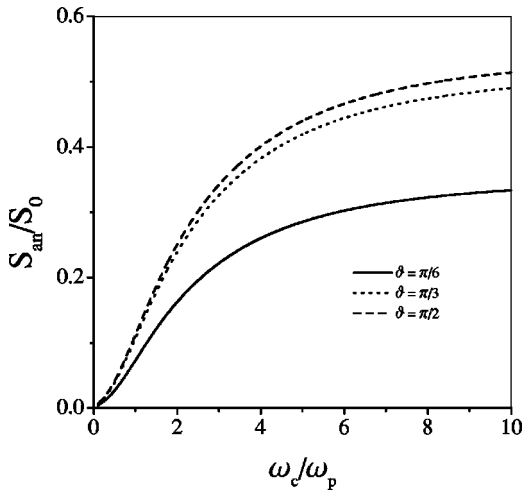

FIG. 10. The ratio of the anomalous stopping power to the stopping power without magnetic field ($S_{\rm an}/S_0$) as a function of ω_c/ω_p for $\mathcal{Z}=0.1$, $V/\overline{v}_{\rm th}=0.2$, $\tau=0.1$, $\vartheta=\pi/6$ (solid line), $\pi/3$ (dotted line), and $\pi/2$ (dashed line).

The anomalous friction coefficient [see Eq. (53)] vanishes, however, when the ion moves along the magnetic field ($\vartheta=0$). Then the friction coefficient is solely given by the second term of Eq. (50). The contribution of this term to the stopping power leads to the usual friction law in plasmas and reads for arbitrary angles ϑ

$$S\simeq\left(\frac{2}{\pi}\right)^{1/2}\frac{2Z^2e^2}{\lambda_{D\parallel}^2}\frac{V}{v_{\rm th\parallel}}\int_0^{\xi_\parallel}k^3dk\int_0^1\frac{d\mu}{\mu}\frac{E_1(k,\mu)}{[k^2+E_2(k,\mu)]^2} \times[\mu^2\cos^2\vartheta+\tfrac{1}{2}(1-\mu^2)\sin^2\vartheta] \tag{58}$$

with

$$E_1(k,\mu)=\sum_{n=1}^{\infty}\Lambda_n(z)\exp\left(-\frac{n^2\eta^2}{2k^2\mu^2}\right)\left[1+\left(\frac{1}{\tau}-1\right)\frac{n^2\eta^2}{k^2\mu^2}\right] \tag{59}$$

and $E_2(k,\mu)$ as defined by Eq. (52).

In Figs. 10 and 11 we compare the anomalous term $S_{\rm an}$ with the low-velocity stopping without magnetic field, S_0 [see Eq. (19)], where $S_{\rm an}/S_0$ is plotted as a function of ω_c/ω_p for $\vartheta=\pi/6$ (solid line), $\pi/3$ (dotted line), and $\pi/2$ (dashed line), $\mathcal{Z}=0.1$, $V/\overline{v}_{\rm th}=0.2$, and for two values of the anisotropy parameter τ: $\tau=0.1$ (Fig. 10) and 10 (Fig. 11).

We conclude that the anomalous term $S_{\rm an}$ gives an important contribution to the stopping, especially for strong magnetic fields ($\omega_c>\omega_p$) and for large temperature anisotropies

($T_\perp \gg T_\parallel$). It should be noted that the observed enhancement of stopping due to S_{an} for $T_\perp \gg T_\parallel$ is potentially interesting for future electron cooling experiments. We note that the appearance of the anomalous term (53), but not its size, is independent of the cutoff (9).

VII. SUMMARY

The purpose of this work was to investigate the stopping power of an ion in a classical magnetized anisotropic two-temperature plasma. A general expression obtained for the stopping power was analyzed in four particular cases: in a plasma without magnetic field; in a plasma with weak and very strong magnetic fields; and in a plasma with arbitrary magnetic field and for low-velocity projectile.

From the results obtained in Secs. III–V, we found that the stopping power essentially depends on the plasma temperature anisotropy. In the field-free case and for small ion velocities, the anisotropy results in an enhancement of the stopping power when the ion moves in the direction with low temperature. For small projectile velocities a weak magnetic field slightly decreases the field-free stopping power for small τ; in the opposite case (large τ) the field-free stopping power slightly increases. In the high-velocity limit the correction to the field-free stopping power for weak magnetic fields is always negative and the stopping power is reduced by the magnetic field. In the case of strong magnetic fields we demonstrated an enhancement of the stopping power with increasing ϑ for low- and high-velocity regions compared to the case of an ion which moves along $\mathbf{B}_0$.

In the low-velocity limit but for arbitrary magnetic field, we found an enhanced stopping power compared to the field-free value, mainly due to the strong coupling between the spiral motion of the electrons and the long-wavelength, low-frequency fluctuations excited by the projectile ion. This anomalous stopping power increases with the angle ϑ (between the ion velocity $\mathbf{V}$ and the magnetic field $\mathbf{B}_0$) and depends strongly on the temperature anisotropy $\tau = T_\perp / T_\parallel$, as seen in Figs. 10 and 11. Although the nature of the anomalous stopping power is only conditioned by the external magnetic field, the temperature anisotropy of the plasma can intensify this effect when $T_\perp \gg T_\parallel$ (see Fig. 11).

This emphasizes the importance of the special role of fluctuations with small $k_\parallel$ and small ω (small projectile velocity V) and as another significant contribution to the energy exchange processes arising from the collective modes of plasma. Potentially, the electron plasma waves and the ion acoustic waves in a magnetized plasma might provide a significant energy-exchange mechanism between projectile ion and plasma particles. This fact makes it necessary to consider the influence of plasma collective modes on the anomalous stopping process. This problem will be treated in a subsequent work.

ACKNOWLEDGMENTS

It is our pleasure to thank Professor Christian Toepffer for helpful discussions. One of the authors (H.B.N.) is grateful for hospitality at the Institut für Theoretische Physik II, Universität Erlangen-Nürnberg, where this work was concluded, and would like to thank the Deutscher Akademischer Austauschdienst for financial support.

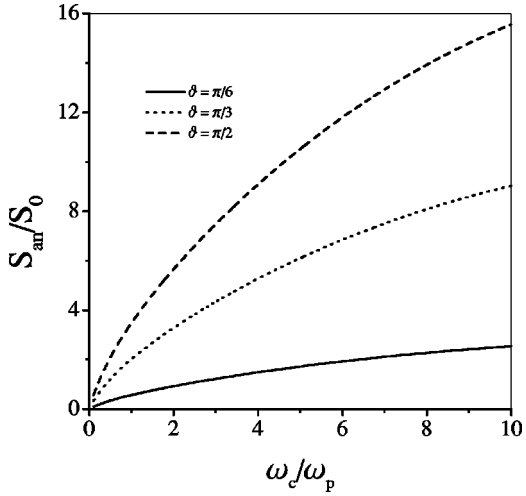

FIG. 11. As Fig. 10, but here $\tau = 10$.

APPENDIX A

Here we describe the evaluation of the dielectric function in the temperature anisotropic case where the velocity distribution of the unperturbed distribution function is given by Eq. (4). We next introduce the Fourier transformations of $f_1(\mathbf{r},\mathbf{v},t)$ with respect to variables $\mathbf{r}$ and t, $f_1(\mathbf{k},\omega,\mathbf{v})$. Because of the cylindrical symmetry (around the magnetic field direction $\mathbf{b} = \mathbf{B}_0/B_0 = \hat{\mathbf{z}}$) of the problem, we choose

$$\mathbf{v} = v_\perp \cos\sigma\hat{\mathbf{x}} + v_\perp \sin\sigma\hat{\mathbf{y}} + v_\parallel\hat{\mathbf{z}}. \tag{A1}$$

Then the Vlasov Eq. (2) for the distribution function becomes

$$\frac{\partial}{\partial\sigma} f_1(\mathbf{k},\omega,\mathbf{v}) + \frac{i}{\omega_c}(\mathbf{k}\cdot\mathbf{v} - \omega - i0) f_1(\mathbf{k},\omega,\mathbf{v}) = -\frac{ie}{m\omega_c}\varphi(\mathbf{k},\omega)\left(\mathbf{k}\frac{\partial f_0}{\partial \mathbf{v}}\right), \tag{A2}$$

where $\varphi(\mathbf{k},\omega)$ is the Fourier transformation of $\varphi(\mathbf{r},t)$. The positive infinitesimal $+i0$ in Eq. (A2) serves to assure the adiabatic turning on of the disturbance and guarantees thereby the causality of the response. The solution of Eq. (A2) has the form

$$f_1(\mathbf{k},\omega,\mathbf{v}) = -\frac{ie}{m\omega_c}\varphi(\mathbf{k},\omega)\int_\infty^\sigma d\sigma_2 \left(\mathbf{k}\frac{\partial f_0}{\partial \mathbf{v}}\right)_{\sigma=\sigma_2} \times \exp\left(\frac{i}{\omega_c}\int_\sigma^{\sigma_2} d\sigma_1[-\omega - i0 + (\mathbf{k}\cdot\mathbf{v})_{\sigma=\sigma_1}]\right). \tag{A3}$$

Combining Eq. (A3) with the Poisson equation (3) we find for the dielectric function

$$\varepsilon(\mathbf{k},\omega)=1-\frac{4\pi i e^2}{m\omega_c k^2}\int_0^\infty v_\perp dv_\perp\int_0^{2\pi}d\sigma\int_{-\infty}^{+\infty}\times dv_\parallel\int_\infty^\sigma d\sigma_2\left(k_\parallel\frac{\partial f_0}{\partial v_\parallel}+k_\perp\cos(\varphi-\sigma_2)\frac{\partial f_0}{\partial v_\perp}\right)\times\exp\left(\frac{i}{\omega_c}\int_\sigma^{\sigma_2}d\sigma_1[k_\parallel v_\parallel-\omega-i0+k_\perp v_\perp\times\cos(\varphi-\sigma_1)]\right),\tag{A4}$$

where $k_x=k_\perp\cos\varphi$, $k_y=k_\perp\sin\varphi$. After integration by the variables σ_1, σ_2, and σ, and using the expression [20]

$$\exp(-iz\sin\theta)=\sum_{n=-\infty}^{+\infty}J_n(z)\exp(-in\theta),\tag{A5}$$

where J_n is the Bessel function of the nth order, we obtain the expression [17]

$$\varepsilon(\mathbf{k},\omega)=1-\frac{8\pi^2e^2}{mk^2}\sum_{n=-\infty}^{+\infty}\int_0^\infty v_\perp dv_\perp\int_{-\infty}^{+\infty}dv_\parallel\left(\frac{n\omega_c}{v_\perp}\frac{\partial f_0}{\partial v_\perp}+k_\parallel\frac{\partial f_0}{\partial v_\parallel}\right)\frac{J_n^2(k_\perp v_\perp/\omega_c)}{n\omega_c+k_\parallel v_\parallel-\omega-i0}.\tag{A6}$$

Substituting Eq. (4) for the unperturbed distribution function f_0 into Eq. (A6) we finally obtain

$$\varepsilon(\mathbf{k},\omega)=1+\frac{1}{k^2\lambda_{D\parallel}^2}\left\{1+\sum_{n=-\infty}^{+\infty}\left(1+\frac{T_\parallel}{T_\perp}\frac{n\omega_c}{\omega-n\omega_c}\right)\times\left[W\left(\frac{\omega-n\omega_c}{|k_\parallel|v_{\mathrm{th}\parallel}}\right)-1\right]\Lambda_n(\beta)\right\},\tag{A7}$$

where $\beta=k_\perp^2v_{th\perp}^2/\omega_c^2=k_\perp^2a_c^2$, $\Lambda_n(z)=\exp(-z)I_n(z)$, $I_n(z)$ is the modified Bessel function of the nth order, and $W(z)$ is the plasma dispersion function [18].

To show the identity of the two forms [Eqs. (6) and (A7)] of the dielectric function we will use the expansion in modified Bessel functions [20]

$$\exp(z\cos\theta)=\sum_{n=-\infty}^{\infty}I_n(z)\exp(in\theta).\tag{A8}$$

This allows us to rewrite $\exp[-X(t)]$ with $X(t)$ from Eq. (7) as

$$\exp[-X(t)]=\exp(-t^2\cos^2\alpha)\sum_{n=-\infty}^{+\infty}\Lambda_n(\beta)\exp\left(\frac{in\omega_c t\sqrt{2}}{kv_{\mathrm{th}\parallel}}\right).\tag{A9}$$

Substituting Eq. (A9) into expression (6) and integrating over the variable t leads to Eq. (A7).

APPENDIX B

We now give a more detail derivation of the anomalous term S_{ar} [Eq. (53)]. We start with the expression

$$Q(k,\varphi,\Lambda)=\int_0^1\frac{d\mu}{\mu}\Phi(\mu,k,\varphi)\exp\left(-\frac{\lambda^2\phi^2(\mu,\varphi)}{2\mu^2}\right)\tag{B1}$$

[see Eq. (51)], where $\phi(\mu,\varphi)=\cos\Theta$, $\lambda=V/v_{\mathrm{th}\parallel}$, and

$$\Phi(\mu,k,\varphi)=\frac{\Lambda_0(z)\cos^2\Theta}{[k^2+E_2(k,\mu)]^2}.\tag{B2}$$

For $\lambda\to0$ a leading-term approximation of Eq. (B1) leads to

$$Q(k,\varphi,\lambda)\simeq\Phi(0,k,\varphi)\ln\frac{\sqrt{2}}{\lambda|\phi(0,\varphi)|\sqrt{\gamma}}+O(1),\tag{B3}$$

where γ is Euler's constant, $|\phi(0,\varphi)|=\sin\vartheta|\cos\varphi|$,

$$\Phi(0,k,\varphi)=\frac{\Lambda_0(k^2\tau/\eta^2)\sin^2\vartheta\cos^2\varphi}{[k^2+E_2(k,0)]^2},\tag{B4}$$

and

$$E_2(k,0)=1+2\left(\frac{1}{\tau}-1\right)\sum_{n=1}^{\infty}\Lambda_n(k^2\tau/\eta^2).\tag{B5}$$

Using the relation [17,20]

$$\sum_{n=-\infty}^{+\infty}\Lambda_n(z)=1,\tag{B6}$$

the function $E_2(k,0)$ finally takes the form

$$E_2(k,0)=\frac{1}{\tau}+\left(1-\frac{1}{\tau}\right)\Lambda_0(k^2\tau/\eta^2).\tag{B7}$$

Substituting Eqs. (B3), (B4), and (B7) into Eq. (51) and integrating over φ, we finally come to expression (53).

[1] A. H. Sørensen and E. Bonderup, Nucl. Instrum. Methods Phys. Res. **215**, 27 (1983).

[2] H. Poth, Phys. Rep. **196**, 135 (1990).

[3] I. N. Meshkov, Fiz. Elem. Chastits At. Yadra **25**, 1487 (1994) [Phys. Part. Nuclei **25**, 631 (1994)].

[4] *Proceedings of the 12th International Symposium on Heavy Ion Inertial Fusion, Heidelberg, 1997* [Nucl. Instrum. Methods Phys. Res. A **415** (1998)].

[5] I. A. Akhiezer, Zh. Eksp. Teor. Fiz. **40**, 954 (1961) [Sov. Phys. JETP **13**, 667 (1961)].

[6] N. Honda, O. Aona, and T. Kihara, J. Phys. Soc. Jpn. **18**, 256 (1963).

[7] R. M. May and N. F. Cramer, Phys. Fluids **13**, 1766 (1970).

[8] G. G. Pavlov and D. G. Yakovlev, Zh. Eksp. Teor. Fiz. **70**, 753 (1976) [Sov. Phys. JETP **43**, 389 (1976)].

[9] J. G. Kirk and D. I. Galloway, Plasma Phys. **24**, 339 (1982).

[10] S. V. Bozhokin and É. A. Choban, Fiz. Plazmy **10**, 779 (1984) [Sov. J. Plasma Phys. **10**, 452 (1984)].
[11] H. B. Nersisyan, Phys. Rev. E **58**, 3686 (1998).
[12] H. B. Nersisyan and C. Deutsch, Phys. Lett. A **246**, 325 (1998).
[13] C. Seele, G. Zwicknagel, C. Toepffer, and P.-G. Reinhard, Phys. Rev. E **57**, 3368 (1998).
[14] M. Walter, C. Toepffer, and G. Zwicknagel, Nucl. Instrum. Methods Phys. Res. B (to be published).
[15] E. Lifshitz and L. P. Pitaevskij, *Physical Kinetics* (Pergamon Press, Oxford, 1981).
[16] G. Zwicknagel, C. Toepffer, and P.-G. Reinhard, Phys. Rep. **309**, 117 (1999).
[17] S. Ichimaru, *Basic Principles of Plasma Physics* (Benjamin, Reading, MA, 1973), Sec. 7.4.
[18] D. B. Fried and S. D. Conte, *The Plasma Dispersion Function* (Academic, New York, 1961).
[19] Th. Peter and J. Meyer-ter-Vehn, Phys. Rev. A **43**, 1998 (1991).
[20] I. S. Gradshteyn and I. M. Ryzhik, *Table of Integrals, Series and Products* (Academic, New York, 1980).